Bayesian Analysis Application in Nuclear Physics

Parada. T. P. Hutauruk
Asia Pacific Center for Theoretical Physics, Gyeongbuk, 36765, South Korea

Keywords: Bayesian Analysis, Kaon Photo-production, Nested Sampling Integration, Excited Baryon Resonances, Associated Legendre Polynomial.

Abstract: Bayesian analysis is applied to analyze the CLAS experimental data of the angular distributions of the differential cross sections, and $C_{x'}$ and $C_{z'}$ double polarizations for $\gamma + p \rightarrow K^+ + \Lambda$ reaction. These observables can be classified into four Legendre classes and represented by associated Legendre polynomial function itself. In this analysis, we intend to determine the best data model for both observables. We use the Bayesian technique to select the best model by calculating the posterior probabilities and comparing the posterior among the models for each observable. The posteriors probabilities for each data model are computed using a Nested sampling integration. From this analysis, we found that the CLAS data set needs no more than four associated Legendre polynomials to describe the differential cross section data. For $C_{x'}$ and $C_{z'}$ double polarizations require two and three order of associated Legendre polynomials respectively to describe the data well. The extracted coefficients of each observable of the best model are presented. It shows the structure of baryon resonances qualitatively.

1 INTRODUCTION

Significant information on the structure of the nucleon can be obtained by studying its excitation spectrum [1, 2]. Over the last few decades, a large amount information about the spectrum of the nucleon has been collected. Most of this information has been extracted from pion-induced and pion photo-production reactions [3, 4]. However, pionic reactions may have biased the information on the existence of certain resonances. Constituent quark model calculations predict a much richer resonance spectrum than that has been observed in pion production experiments [8]. Predicted resonances which have not been observed are called "missing" resonances. Instead, the constituent quark model (CQM) also predicts that these "missing" resonances may couple strongly to KΛ and KΣ channels or other final states involving vector mesons [8, 9, 10]. Since performing kaon-hyperon, kaon-nucleon or hyperon-nucleon scattering experiments is a daunting task, kaon photo-production on the nucleon appears to be a good alternative solution [9, 10].

Experiments on kaon photo-production and electro-production started in the 1960s[11]. However, the old experimental data are often inconsistent and have large error bars. In recent years, a large amount of data for kaon photo-production has been collected. High statistics data from the CLAS, for differential cross sections, recoil polarization, C_x and C_z double polarizations for the reaction $\gamma + p \rightarrow K^+ + \Lambda$ have been published since several years ago [12, 13]. The world database for the reaction $\gamma + p \rightarrow K^+ + \Lambda$ is more available now. This gives a possibility to analyze the data more accurately. Recently the newest experimental data for the $K^+\Lambda$ channel of photon asymmetry (Σ), target polarization (T), recoil polarization (P), and $O_{x'}$ and $O_{z'}$ double polarizations has been collected [14]. Unfortunately, the experimental data do not published yet. Furthermore the experimental data for other observables such as G asymmetry will available soon from Jefferson Lab. Newport News, USA.

Additional experimental data have also been measured by SAPHIR [15, 16, 17], LEPS [18, 19] and GRAAL [20]. Several previous analyses have been applied to the results of these experiments, such as Isobar models [9, 10, 21, 22, 23] and Coupled channel models [24, 25, 26]. However different theoretical model calculations often produce very different predictions.

Based on paper of Ref.[5], all sixteen observables in kaon photo-production were shown to be classified into the classes $\mathscr{L}_0\left(\hat{\mathbf{I}};\ \hat{\mathbf{E}};\ \hat{\mathbf{C}_{\mathbf{z'}}};\ \hat{\mathbf{L}_{\mathbf{z'}}}\right)$,

Hutauruk, P.
Bayesian Analysis Application in Nuclear Physics.
DOI: 10.5220/0008908700002481
In *Proceedings of the Built Environment, Science and Technology International Conference (BEST ICON 2018)*, pages 310-315
ISBN: 978-989-758-414-5

$\mathscr{L}_{1a}\left(\hat{\mathbf{P}};\ \hat{\mathbf{H}};\ \hat{\mathbf{C}_{\mathbf{x}'}};\ \hat{\mathbf{L}_{\mathbf{x}'}}\right)$, $\mathscr{L}_{1b}\left(\hat{\mathbf{T}};\ \hat{\mathbf{F}};\ \hat{\mathbf{O}_{\mathbf{x}'}};\ \hat{\mathbf{T}_{\mathbf{z}'}}\right)$, and $\mathscr{L}_{2}\left(\hat{\mathbf{\Sigma}};\ \hat{\mathbf{G}};\ \hat{\mathbf{O}_{\mathbf{z}'}};\ \hat{\mathbf{T}_{\mathbf{x}'}}\right)$, where each class is an expansion in a different set of associated Legendre polynomials. What is not apparent is how many terms in each expansion are required. This work attempts to address the issue by examining data models with different numbers of terms, and calculating which one has the greatest posterior probability. In this article we focus on the differential cross section observables, which are described by the associated Legendre class $\mathscr{L}_0$ and the double polarizations of $C_{x'}$ and $C_{z'}$, which are described by the associated Legendre class $\mathscr{L}_0$ and $\mathscr{L}_{1a}$, respectively.

This paper is organized as follows. We begin with a brief review on the Bayesian analysis procedure which contains the data model and model comparison in Sec. 2. Then in Sec. 3 our numerical results are presented and their implications are discussed. Sec. 4 is devoted for a summary.

2 ANALYSIS PROCEDURE

In this section, the Bayesian analysis [6] procedure for the kaon photo-production is presented. We begin to construct the data model based on the Legendre classes. We then use a comparison strategy to determine the best model. In general we have two steps to determine the best model. Firstly to compute the maximum posterior for each photon energy for each observable. Secondly to compare the maximum posterior among the models with different order of Legendre polynomials. We then employ the Nested sampling integration to execute the multi-integral over the parameters of Legendre polynomials. Nested sampling is a very powerful technique to evaluate the multi-dimensions integral into one dimension integral. This also has been used in many fields such as astrophysics [27], cosmology [28], statistics [29], and high energy physics [30].

2.1 Data Model

We construct data models based on Legendre class $\mathscr{L}_0$. These data models can be written compactly as follows:

$$M_L^{\mathscr{L}_0} = \sum_{l=0}^{l=L} A_l P_{l0}(\cos\theta). \tag{1}$$

where $M_L^{\mathscr{L}_0}$ is the data model, and A_l and $P_{l0}(cos\theta)$ are the coefficients and associated Legendre polynomials, respectively. Each data model therefore has a different "order" or maximum number of polynomials. Our task is to find the most likely order. Note that analogous data model can be built for another Legendre class.

2.2 Model Comparison

To determine the best model, we evaluate the posterior probability [6] for each data model. The ratio of the probabilities for M_L and M_0 can be written, using Bayes theorem, as follows :

$$R = \frac{P(M_L|D)}{P(M_0|D)} = \frac{P(D|M_L)}{P(D|M_0)} \times \frac{P(M_L)}{P(M_0)}. \tag{2}$$

where $P(M_L|D)$ is the posterior for the M_L model, $P(D|M_L)$ is the probability that the data would be obtained, assuming M_L to be true (the likelihood). With no prior prejudice as to which variant is correct, we obtain the ratio of likelihoods:

$$R = \frac{P(D|M_L)}{P(D|M_0)}$$

The likelihood $P(D|M_L)$ is an integral over the joint likelihood $P(D,\{A_l\}|M_L)$, where $\{A_l\}$ represents a set of free parameters:

$$\begin{aligned} P(D|M_L) &= \int ... \int P(D,\{A_l\}|M_L) d^L A_l, \\ &= \int ... \int P(D|\{A_l\},M_L) P(\{A_l\}|M_L) d^L A_l. \end{aligned} \tag{3}$$

The function $P(A_l|M_L)$ is the prior probability that the parameters take on specific values. We assume that each parameter A_l lies in the range $A_l^{min} \leq A_l \leq A_l^{max}$, and we can write the prior as the reciprocal of the volume of a hyper-cube in parameter search space as $P(\{A_l\}|M_L) = \frac{1}{\prod^L (A_l^{max} - A_l^{min})}$. If the errors in the data points are Gaussian, it can be shown that $P(D|\{A_l\},M_L) \propto \exp\left(-\frac{\chi^2}{2}\right)$, where χ^2 is the sum of squared residuals. Using a Taylor series expansion about the minimum χ^2 , $\chi^2 \approx \chi^2_{min} + \frac{1}{2}(\mathbf{X} - \mathbf{X_0})^T \nabla^2 \chi^2 (\mathbf{X} - \mathbf{X_0}) + ...$, we can write an approximate form for the likelihood:

$$P(D|M_L) \propto \frac{L!(4\pi)^L}{\prod^L (A_l^{max} - A_l^{min}) \times \sqrt{Det(\nabla\nabla\chi^2)}} \exp\left(-\frac{\chi^2_{min}}{2}\right). \tag{4}$$

where L is the dimension of the integral and $(Det(\nabla\nabla\chi^2)$ is the determinant of the Hessian matrix, which in turn is the inverse of the covariance matrix.

For simplicity the Eq.(3) can also be written as follows:

$$\mathcal{Z} = \int \mathcal{L}(\mathbf{A_i}) \pi(\mathbf{A_i}) d\mathbf{A_i}. \tag{5}$$

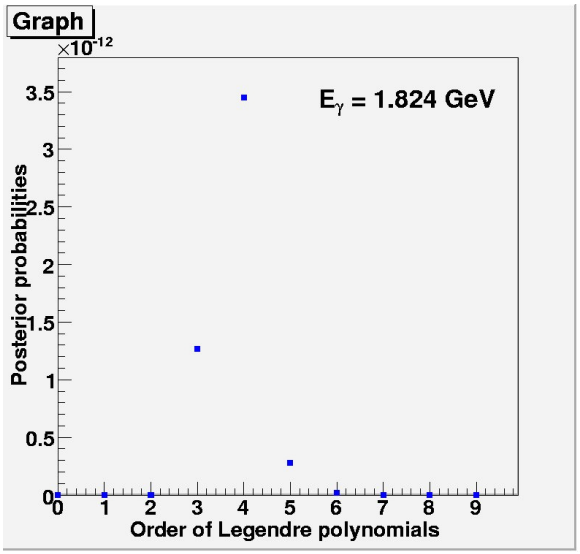

Figure 1: The posterior probabilities for different orders of data model, for E_γ = 1.824 GeV.

Where $\mathcal{L}(\mathbf{A_i})$ is the likelihood functions and $\pi(\mathbf{A_i})$ is the prior distribution. Nested sampling is a Monte Carlo integration technique for evaluating the integral of a likelihood function or Bayesian Evidence in Eq.(5) over its range of parameters which is developed by Skilling [31]. This technique exploits the relation between the likelihood and prior volume to transform the multidimensional of evidence integral into one dimensional integral. The prior volume X is defined by $dX = \pi(\Theta)d^D_\Theta$, so that:

$$X(\lambda) = \int_{\mathcal{L}(\Theta)} \pi(\Theta) d^D_\Theta, \tag{6}$$

where the integral extend over the region of the parameter space contained the iso-likelihood contour $\mathcal{L}(\Theta) = \lambda$. Assuming that $\mathcal{L}(X)$ is monotonically decreasing function of X which is trivially satisfied for most posteriors. The evidence integral can be written as follows:

$$\mathcal{Z} = \int_0^1 \mathcal{L}(X) dX. \tag{7}$$

A more detailed of this technique can be found in Ref. [31].

3 NUMERICAL RESULTS

Using the above analysis procedure, for each of the available photon energy bins, we fitted each data

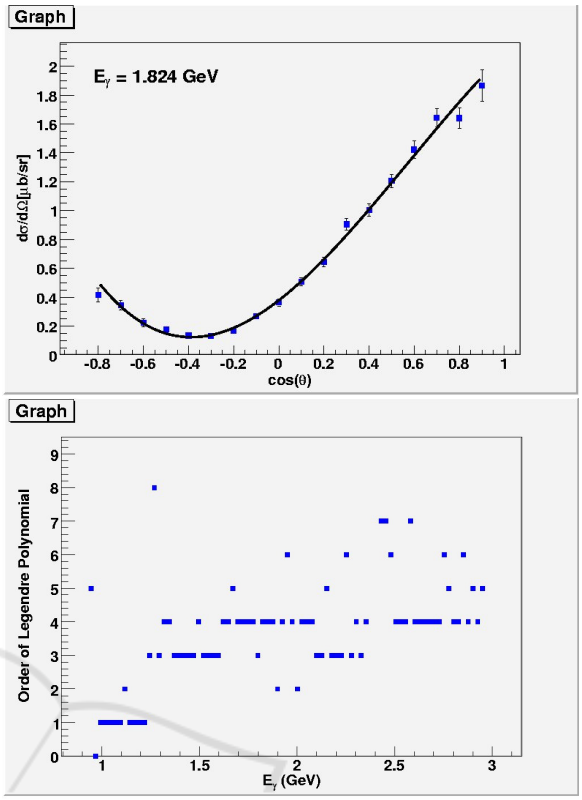

Figure 2: Plot showing the fit of the fourth order data model to the CLAS cross section data for E_γ = 1.824 GeV (on the top).The order of associated Legendre polynomial for all photon energy (on the bottom).

model to the angular distribution. This was carried out using the standard minimization package MINUIT. We then compared models with different numbers of Legendre polynomials by evaluating Eq. (4) for each data model.

To illustrate the procedure, we first choose one photon energy bin at E_γ = 1.824 GeV as an example. The posterior probabilities are shown in Fig. 1, where the order of the data model is shown on the horizontal axis. The maximum posterior is given by the data model containing four associated Legendre polynomials.

On the left side in Fig. 2 we show the fit of the fourth order data model to the CLAS differential cross section data [12] for E_γ = 1.824 GeV. The procedure is repeated for each photon energy bin. The right side in Fig. 2 the order of data model which has the greatest probability at each photon energy is plotted. It can be seen that this generally increase from threshold into the resonance region, but that the maximum is mostly at the fourth order. The distributions of the polynomial coefficients for fourth order data models

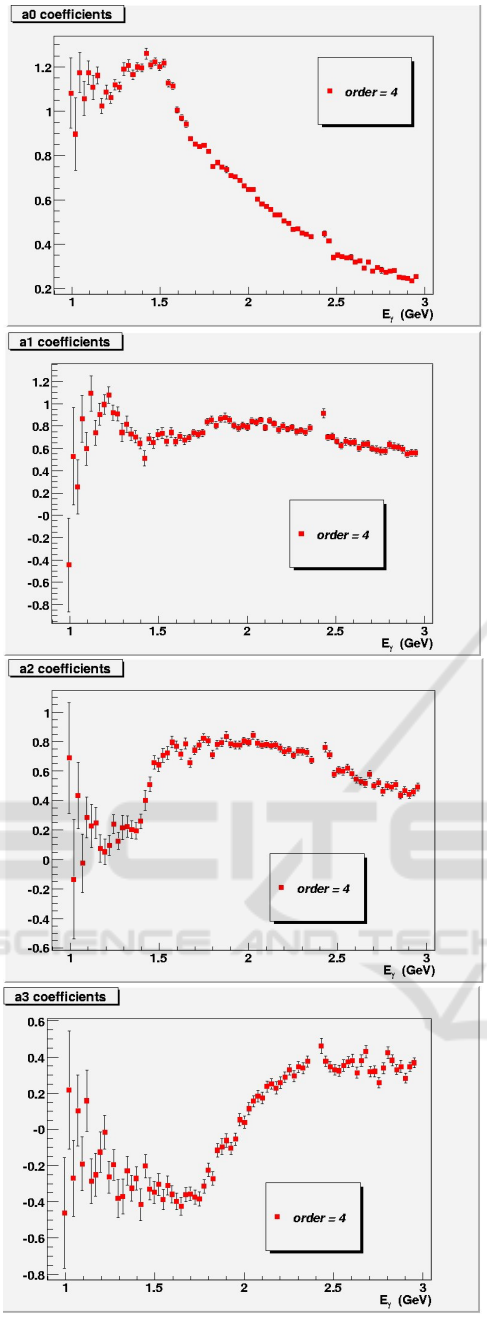

Figure 3: Extracted associated Legendre polynomial coefficients for each photon energy.

as a function of photon energy is shown in Fig. 3.

The experimental data available for $K\Lambda$ of C_x dan C_z double polarization measured at unprime coordinate system, whereas in our analysis we require the data of $C_{x'}$ and $C_{z'}$ double polarization which were measured at prime coordinate system (outgoing kaon or z'-axis). Hence we have to transform these observables using a standard rotation matrix as follows:

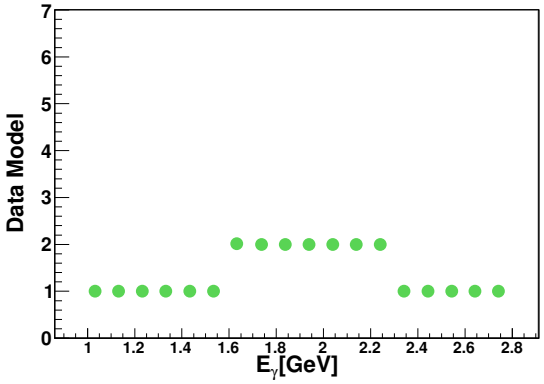

Figure 4: The best data model for each photon energy for $C_{x'}$ double polarization.

$$C_{x'} = C_x \cos\theta - C_z \sin\theta,$$
$$C_{z'} = C_x \sin\theta + C_z \cos\theta. \quad (8)$$

Where θ is the kaon scattering angle. Then the results of this transformation will be used in the analysis.

Using Eq. (7) we computed the evidence for each photon energies (E_γ). For calculating the posterior we chosen the uniform prior distribution $\pi(\Theta)$. We then compared the posterior of the data model with different order of associated Legendre polynomials for each photon energies. The best data model for each photon energy of $C_{x'}$ double polarization are shown in Fig. 4. Fig. 4 provides most experimental data of $C_{x'}$ double polarization can be described well by M_1 data model. Extracted coefficients of the best model for $C_{x'}$ double polarization provided in Fig. 6. The extracted coefficients results for other models are also shown in Fig. 6.

With similar procedures, the best data model for $C_{z'}$ double polarization are shown in Fig. 5. The most experimental data for $C_{z'}$ double polarization can described by M_2 data model. The extracted coefficients for this observable provided in Fig. 7. Generally the extracted coefficients results of the best data model for $C_{x'}$ and $C_{z'}$ double polarizations may reveal the baryon resonances.

4 SUMMARY

Bayesian analysis is a powerful tools for determining the best data model. We have analyzed the Legendre polynomial decomposition of differential cross section data and the associated Legendre polynomials of $C_{x'}$ and $C_{z'}$ double polarizations data. We generated data models with different numbers of associated

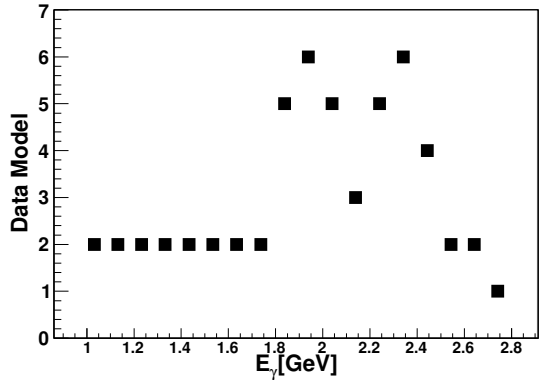

Figure 5: The best data model for each photon energy for $C_{z'}$ double polarization.

Legendre polynomials. We computed the evidence of the data models by using the Nested sampling integration. We then compared them by calculating posterior probabilities. From this analysis, we found that differential cross section data in this case requires at least four associated Legendre polynomials, and $C_{x'}$ and $C_{z'}$ double polarizations require two and three order of associated Legendre polynomials respectively.

ACKNOWLEDGMENTS

P .T .P .H is supported by the Ministry of Science and Education, ICT and transportation, Pohang city, Gyeongsangbukdo, South Korea.

REFERENCES

[1] M. Guidal, J. M. Laget and M. Vanderhaeghen, Nucl. Phys. A **627**, 645 (1997).

[2] N. Kaiser, T. Waas and W. Weise, Nucl. Phys. A **612**, 297 (1997).

[3] J. A. Mueller [CLAS Collaboration],Nucl. Phys. A **721**, 701 (2003).

[4] D. Sokhan *et al.* [CLAS Collaboration], Int. J. Mod. Phys. A **24**, 497 (2009).

[5] C. G. Fasano and Frank Tabakin, Phys. Rev. C**64**, 6 (1992).

[6] D. S. Sivia, Data Analysis: A Bayesian Tutorial. Clarendon Press. Oxford. (1996).

[7] R. A. Adelseck and B. Saghai, Phys. Rev. C**42**, 108 (1990).

[8] S. Capstick and W. Roberts, Phys. Rev. D**49**, 4570 (1994).

[9] T. Mart and C. Benhold, Phys. Rev. C **61**, 012201R (2000).

[10] T. Mart, Phys. Rev. C **62**, 038201 (2000).

[11] E. G. Gorzhevskaya, V. M. Popova and F. R. Yagudina, Sov. Phys. JETP **11**, 200 (1960) [Zh. Eksp. Teor. Fiz. **38**, 276 (1959)].

[12] R. Bradford *et al.* (CLAS collaboration), Phys. Rev. C **73**, 035202 (2006).

[13] R. Bradford *et al.* (CLAS collaboration), Phys. ReV. C**75**, 035205 (2007).

[14] Craig Patterson, PhD Thesis, University of Glasgow, Scotland 2008 (unpublished).

[15] K. -H. Glander *et al.* (SAPHIR collaboration), Eur. Phys. J. A**19**, 251-273 (2004).

[16] M. Q. Tran *et al.* (SAPHIR collaboration), Phys. Lett. B**445**, 20 (1998).

[17] K. -H. Glander *et al.* (SAPHIR collaboration), Nucl. Phys. A**754**, 294c-302c (2005).

[18] M. Sumihama *at al.* (LEPS collaboration), Phys. Rev. C**73**, 035214 (2006).

[19] R. G. T. Zegers *et al.* (LEPS collaboration), Phys. Rev. Lett. **91**, 9 (2003).

[20] A. Lleres *et al.* (GRAAL collaboration), Eur. Phys. J. A**31**, 79-93 (2007).

[21] D. G. Ireland, S. Janssen, J. Ryckebusch, Nucl. Phys. A**740**, 147-167 (2004).

[22] Stijn Janssen *et al*, Phys. Rev. C**65**,015201 (2001).

[23] S. Janssen *et al.*, Eur. Phys. J. A**11**, 105-111 (2001).

[24] V. Shklyar *et al.*, Phys. Rev. C**71**, 055206 (2005)and references therein.

[25] A. Usov and O. Scholten, Phys. Rev. C**72**, 025205 (2005).

[26] G. Penner and U. Mosel, Phys. Rev. C**66**, 055211 (2002).

[27] Pia Mukherjee, David Parkinson and Andrew R. Liddle, Astrophys. J. **638** (2006) L51-L54.

[28] R. Trotta, arXiv:1701.01467 [astro-ph.CO].

[29] W. K. Hastings, Biometrika **57**, 97 (1970).

[30] G. D'Agostini, CERN-99-03, CERN-YELLOW-99-03.

[31] J. Skilling, Bayesian Analysis **4**(2006) 883-860.

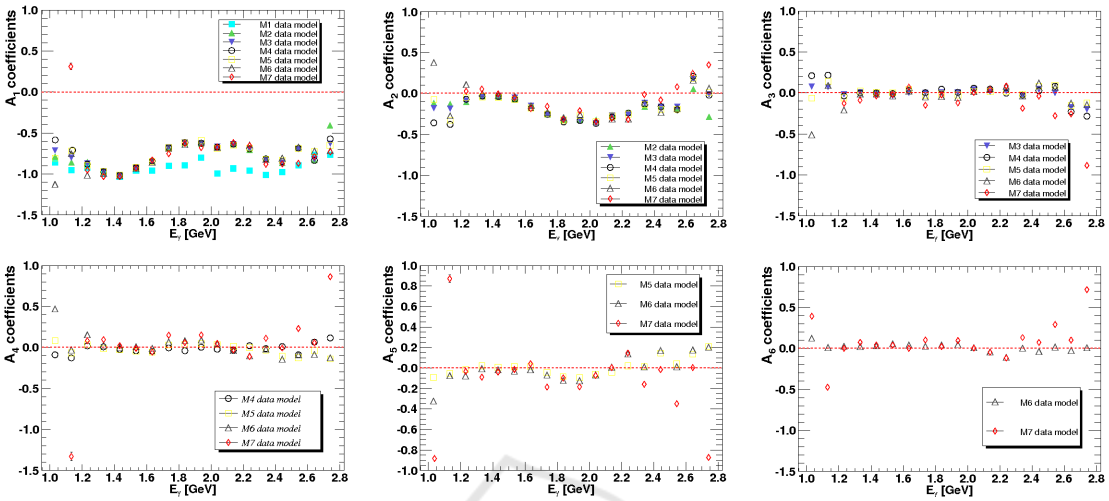

Figure 6: Extracted coefficients of $C_{x'}$ double polarization for each photon energies.

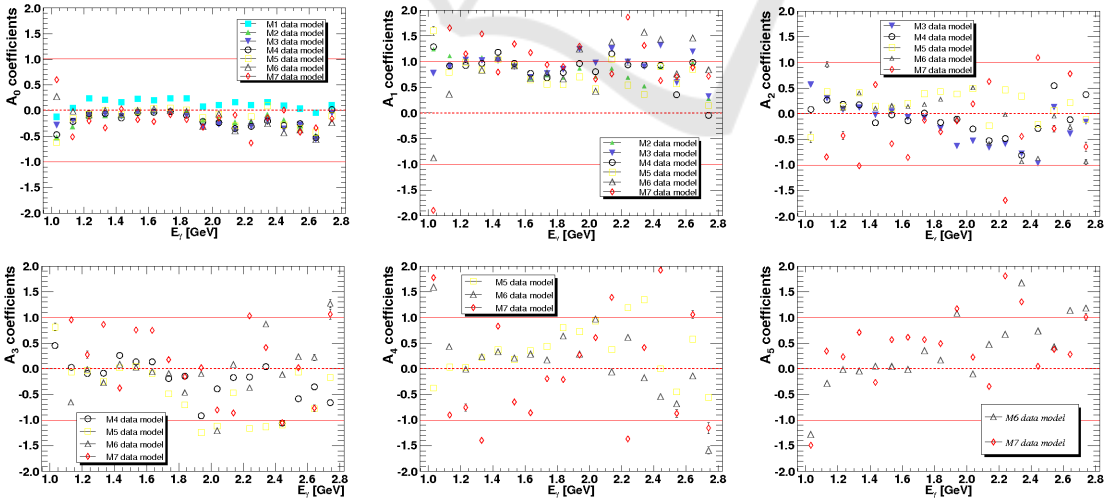

Figure 7: Extracted coefficients of $C_{z'}$ double polarization for each photon energies.